CHIN. PHYS. LETT. Vol. 32, No. 10 (2015) 106101

Magneto-Caloric Response of a $Gd_{55}Co_{25}Al_{18}Sn_2$ Bulk Metallic Glass *

DING Ding(丁鼎)**, ZHANG Yi-Qing(张一清), XIA Lei(夏雷)

Laboratory for Microstructure, Institute of Materials, Shanghai University, Shanghai 200072

(Received 21 May 2015)

The magneto-caloric effect (MCE) of a $Gd_{55}Co_{25}Al_{18}Sn_2$ bulk metallic glass (BMG) is investigated. The $Gd_{55}Co_{25}Al_{18}Sn_2$ as-cast rod prepared by a water-cooled copper mold suction casting method exhibits typical amorphous characteristics. The maximum magnetic entropy change ($-\Delta S_{\rm m}^{\rm peak}$) and the magnetic refrigerant capacity ($R_{\rm C}$) of the BMG under a field of 5 T are about 9.32 J·kg^{-1}·K^{-1} and 832 J·kg^{-1}, respectively, both of which are larger than the values of the $Gd_{55}Co_{25}Al_{20}$ BMG. The mechanism for the improved MCE by minor Sn addition is studied and the field dependence of $-\Delta S_{\rm m}^{\rm peak}$ is investigated for a better understanding on the magneto-caloric behaviors of $Gd_{55}Co_{25}Al_{18}Sn_2$ BMG.

PACS: 61.43.Dq, 81.05.Kf, 75.30.Sg, 81.20.−n DOI: 10.1088/0256-307X/32/10/106101

Magnetic refrigeration (MR) has attracted tremendous attention in the last decade due to the fact that it is regarded as an environmentally friendly and highly efficient technology.[1,2] As a basis of MR, magneto-caloric effect (MCE) is the exothermic and endothermic effect of a magnetic material upon the application and removal of a magnetic field. MCE of materials was usually evaluated by two parameters: the peak value of magnetic entropy change $-\Delta S_{\rm m}^{\rm peak}$ and the refrigeration capacity $R_{\rm C}$.[3] Bulk metallic glasses (BMGs) have aroused interest as suitable candidates for magnetic refrigerants due to their unique properties, such as excellent soft magnetic properties, large electrical resistivity, high corrosion resistance and outstanding mechanical properties.[4–7] On the other hand, in contrast to most of the crystalline materials,[8–10] amorphous materials show a broadened magnetic entropy change peak due to the second magnetic phase transition they undergo near the Curie temperature ($T_{\rm c}$), which leads to an ultrahigh $R_{\rm C}$.[11–25] Unfortunately, the BMGs possess relatively low $-\Delta S_{\rm m}^{\rm peak}$ at the same time. Thus to improve $-\Delta S_{\rm m}^{\rm peak}$ of the BMGs is one of the key challenges for the application of these BMGs as magnetic refrigerants.

In this Letter, we attempt to improve the MCE of the $Gd_{55}Co_{25}Al_{20}$ BMG[26] by minor Sn addition as a replacement of Al. The values of $-\Delta S_{\rm m}^{\rm peak}$ and $R_{\rm C}$ of the $Gd_{55}Co_{25}Al_{18}Sn_2$ BMG are obtained from the isothermal magnetization curves measured from 20 K to 180 K. It is found that both $-\Delta S_{\rm m}^{\rm peak}$ and $R_{\rm C}$ of the $Gd_{55}Co_{25}Al_{18}Sn_2$ BMG are larger than those of the $Gd_{55}Co_{25}Al_{20}$ BMG, indicating the enhanced MCE by minor Sn substitution. The mechanism of the improved MCE by minor Sn addition is investigated. The field dependence of $-\Delta S_{\rm m}^{\rm peak}$ for the $Gd_{55}Co_{25}Al_{18}Sn_2$ BMG is constructed to understand the magneto-caloric behaviors of the BMG in more detail.

In our experiment, a $Gd_{55}Co_{25}Al_{18}Sn_2$ ingot was prepared by arc melting of 99.9% (at%) pure Gd, Co, Al, Sn elements in a water-cooled copper crucible under a Ti-gettered argon atmosphere. An as-cast rod with a diameter of 2 mm was fabricated by suction casting the melt into a water-cooled copper mold under the same argon atmosphere. The amorphous characteristics of the as-cast rod were ascertained by x-ray diffraction (XRD) using a Rigaku D/max2550 diffractometer with Cu K_α radiation and a Perkin–Elmer diamond differential scanning calorimeter (DSC) at a heating rate of 20 K/min. The magnetic properties of $Gd_{55}Co_{25}Al_{18}Sn_2$ BMG were measured by a quantum design physical properties measurement system (PPMS): the magnetic hysteresis loops were measured at 10 K and 300 K under a field of 5 T; the temperature dependence of magnetization (M–T) was measured from 10 K to 300 K under a field of 0.03 T; and the isothermal magnetization (M–H, H is the magnetic field) curves were measured at different temperatures ranging from 20 K to 180 K under a field of 5 T.

The XRD pattern of the $Gd_{55}Co_{25}Al_{18}Sn_2$ as-cast rod is shown in Fig. 1, and the DSC trace is shown in the inset of Fig. 1. Both the XRD pattern and the DSC trace illustrate a typical amorphous characteristic of the $Gd_{55}Co_{25}Al_{18}Sn_2$ as-cast rod. The onsets of glass transition temperature $T_{\rm g}$ and crystallization temperature T_x of the $Gd_{55}Co_{25}Al_{18}Sn_2$ as-cast rod are about 562 K and 623 K, respectively, both of which are similar to those of the $Gd_{55}Co_{25}Al_{20}$ BMG, indicating the similar thermal properties and glass forming ability of the two BMGs. The parameters, as listed in Table 1, are similar to those of the $Gd_{55}Co_{25}Al_{20}$ BMG (also listed in Table 1), indicating the similar thermal properties and glass forming ability of the two BMGs.[26]

*Supported by the National Natural Science Foundation of China under Grant Nos 51171100 and 51271103.

**Corresponding author. Email: d.ding@shu.edu.cn

© 2015 Chinese Physical Society and IOP Publishing Ltd

Table 1. Thermal and magnetic properties of the $Gd_{55}Co_{25}Al_{20-x}Sn_x$ ($x = 0$ and 2) BMGs.

Properties	T_g (K)	T_x (K)	T_c (K)	μ_{eff} (μB)	M_s under 2 T (A·m^2/kg)	$-\Delta S_m^{peak}$ under 5 T (J·kg^{-1}K^{-1})	R_C under 5 T (J·kg^{-1})
$Gd_{55}Co_{25}Al_{20}$[26]	562.5	629	112.5	7.24	206.5	8.97	798
$Gd_{55}Co_{25}Al_{18}Sn_2$	562	623	112.5	7.63	208	9.32	832

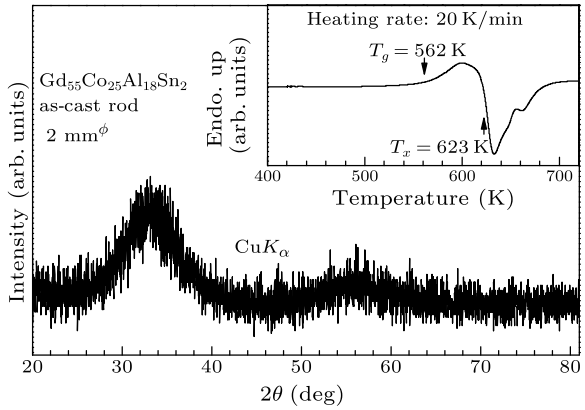

Fig. 1. XRD pattern of $Gd_{55}Co_{25}Al_{18}Sn_2$ as-cast rod. The inset shows the DSC trace of $Gd_{55}Co_{25}Al_{18}Sn_2$ as-cast rod at a heating rate of 20 K/min.

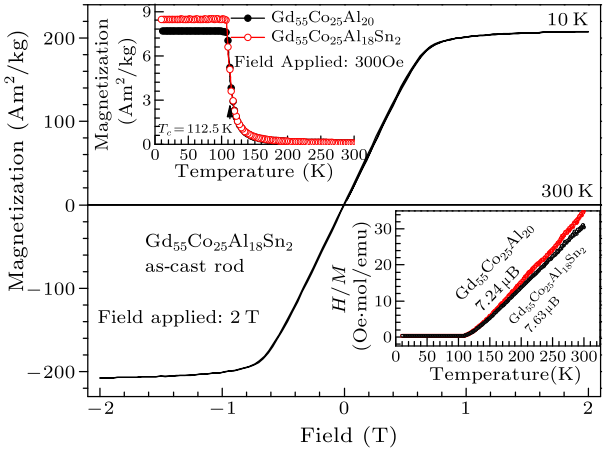

Fig. 2. Magnetic hysteresis loops of the $Gd_{55}Co_{25}Al_{18}Sn_2$ as-cast rod at 300 K and 10 K under a magnetic field of 2 T. The inset shows the M–T curves of the $Gd_{55}Co_{25}Al_{18}Sn_2$ as-cast rod under a field of 0.03 T and the effective moment of $Gd_{55}Co_{25}Al_{18}Sn_2$ and $Gd_{55}Co_{25}Al_{20}$ as-cast rods.

Figure 2 shows the hysteresis loops of $Gd_{55}Co_{25}Al_{18}Sn_2$ as-cast rod measured at 10 K and 300 K, respectively. $Gd_{55}Co_{25}Al_{18}Sn_2$ BMG under a field of 2 T is ferromagnetic at 10 K with a saturation magnetization (M_s) of about 208.0 A·m^2/kg and a nearly zero hysteresis, and is paramagnetic at room temperature. The value of M_s of $Gd_{55}Co_{25}Al_{18}Sn_2$ as-cast rod is slightly higher than that of $Gd_{55}Co_{25}Al_{20}$ BMG (M_s = 206.5 A·m^2/kg).[26] In addition, the improved M_s as well as the nearly zero coercivity suggests enhanced magnetic entropy change due to the enlarged total magnetic moment by the much more complicated microstructure of the BMGs. This shows the M–T curves of $Gd_{55}Co_{25}Al_{18}Sn_2$ and $Gd_{55}Co_{25}Al_{20}$ as-cast rods. The Curie temperature of the $Gd_{55}Co_{25}Al_{18}Sn_2$ BMG (T_c = 112.5 K) has been determined as the temperature at which the absolute value of dM/dT has a peak, which is almost the same as that of the $Gd_{55}Co_{25}Al_{20}$ BMG,[21] as shown in the inset of Fig. 2.

The magnetic entropy change $-\Delta S_m$ can be calculated from the isothermal magnetization curves at different temperatures under a certain magnetic field according to the Maxwell equation. Figure 3(a) shows the temperature dependence of ΔS_m ($(-\Delta S_m)$–T curve) for the $Gd_{55}Co_{25}Al_{18}Sn_2$ BMG under a magnetic field of 5 T, and the curve for $Gd_{55}Co_{25}Al_{20}$ BMG for comparison. Here $-\Delta S_m^{peak}$ of $Gd_{55}Co_{25}Al_{18}Sn_2$ BMG under 5 T is about 9.32 J·kg^{-1}·K^{-1} at T_c (112.5 K), which is about 4% higher than that of the $Gd_{55}Co_{25}Al_{20}$ BMG[26] (about 8.97 J·kg^{-1}·K^{-1} at T_c (112.5 K)), indicating the enhanced $-\Delta S_m^{peak}$ by minor Sn addition. On the other hand, R_c ($=-\Delta S_m^{peak} \times \Delta T_m$, where ΔT_m is the temperature range at the half maximum of $-\Delta S_m^{peak}$) of $Gd_{55}Co_{25}Al_{18}Sn_2$ BMG is about 832 J·kg^{-1} under 5 T, which is also 4.3% higher than that of the $Gd_{55}Co_{25}Al_{20}$ BMG (about 798 J·kg^{-1}) under the same magnetic field. Thus MCE of the $Gd_{55}Co_{25}Al_{20}$ BMG is obviously improved by minor Sn addition.

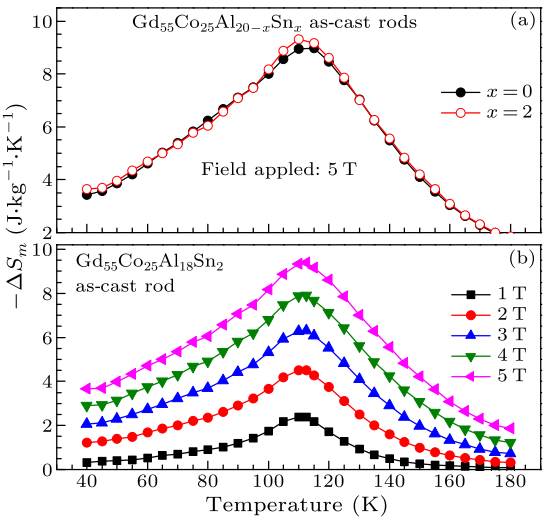

Fig. 3. (a) The $(-\Delta S_m)$–T curves of $Gd_{55}Co_{25}Al_{18}Sn_2$ and $Gd_{55}Co_{25}Al_{20}$ as-cast rods under a field of 5 T. (b) The $(-\Delta S_m)$–T curves of $Gd_{55}Co_{25}Al_{18}Sn_2$ as-cast rod under 1 T, 2 T, 3 T, 4 T and 5 T.

It is known that the entropy changing with the variation of magnetic field depends mainly on the ordering of the magnetic moments of magnetic ma-

terials. Therefore, for a ferromagnetic material, MCE is closely related to the total magnetic moment. However, the nominal magnetic moment of the $Gd_{55}Co_{25}Al_{18}Sn_2$ BMG is equal to that of the $Gd_{55}Co_{25}Al_{20}$ BMG. Considering the strong interaction of the magnetic moment between the Gd element with $4f$-electrons and the Co element with $3d$-electrons, the effective magnetic moment $\mu_{\rm eff}$ (Refs. [27,28]) may be more suitable for the investigation of the mechanism of the enhanced MCE by minor Sn addition. Plots of the ratio H/M as a function of temperature for the $Gd_{55}Ni_{25}Al_{18}Sn_2$ and $Gd_{55}Co_{25}Al_{20}$ BMGs are shown in the inset of Fig. 2. Here $\mu_{\rm eff}$ of the $Gd_{55}Co_{25}Al_{18}Sn_2$ BMG calculated according to the Curie–Weiss law is about 7.63 μB, which is nearly 5% larger than that of the $Gd_{55}Co_{25}Al_{20}$ rod (about 7.24 μB). The enlarged $\mu_{\rm eff}$ in $Gd_{55}Ni_{25}Al_{18}Sn_2$ BMG, which indicates the strengthened $3d$–$4f$ interaction by minor Sn addition, appears to be the mechanism for the improved MCE of $Gd_{55}Ni_{25}Al_{18}Sn_2$ BMG.

The normalized parameters, including the relative magnetic entropy change $-\Delta S_{\rm m}/H$ and the relative cooling power $R_{\rm C}/H$,[29] are usually applied to evaluate the MCE of different materials due to the fact that $-\Delta S_{\rm m}^{\rm peak}$ and $R_{\rm c}$ of the magnetic materials are usually obtained under different magnetic fields in literature. However, according to the $(-\Delta S_{\rm m})$–T curves of the $Gd_{55}Ni_{25}Al_{18}Sn_2$ BMG under different magnetic fields, as shown in Fig. 3(b), the normalized parameters change with the applied field obviously. For example, $R_{\rm C}/H$ for the BMG is about 76.6 J·kg^{-1}T^{-1} under 1 T, 131.35 J·kg^{-1}T^{-1} under 2 T, 141.2 J·kg^{-1}T^{-1} under 3 T, 151.4 J·kg^{-1}T^{-1} under 4 T and 162.1 J·kg^{-1}T^{-1} under 5 T, respectively. Obviously, the normalized parameter is not a constant with the variation of applied field, indicating that the normalized parameters are no longer the valid way for evaluating the MCE obtained under different fields of magnetic materials.

The field dependence of $-\Delta S_{\rm m}$ could be helpful for understanding of the above phenomena. In general, for soft magnetic alloys undergoing a second order magnetic phase transition, the field dependence of $-\Delta S_{\rm m}$ follows a $-\Delta S_{\rm m} \propto H^n$ relationship:[30–32] $n = 1$ at the temperature well below $T_{\rm c}$; $n = 2$ in the paramagnetic range as a result of the Curie–Weiss law; $n \approx 2/3$ near $T_{\rm c}$ derived by Oesterreicher *et al.*[33] according to the mean field theory, or $n \approx 0.72$ near $T_{\rm c}$ according to the Arrott–Noakes equation. The n value near $T_{\rm c}$ can be obtained directly by fitting the $-\Delta S_{\rm m}^{\rm peak}$–$H$ plots, or calculated indirectly by $n(T = T_{\rm c}) = 1 + (\beta - 1)/(\beta + \gamma)$ (Refs. [34,35]) (where β and γ are critical exponents that can be derived from the dc magnetization curves by using the Kouvel–Fisher (K-F) method). Figure 4(a) shows the $\ln(-\Delta S_{\rm m}^{\rm peak})$–$\ln H$ plots of $Gd_{55}Co_{25}Al_{18}Sn_2$ BMG, and thus n can be obtained to be about 0.82, which is similar to that of the other BMGs while much larger than the one predicted by the mean field theory, which is supposed to be attributed to the complicated microstructure of the BMGs with short-range order, medium-range order or even nano-crystallized structures embedded in a disordered matrix.[36] Figure 4(b) shows the Arrott–Noakes (A-N) plots derived from the dc magnetization curves of the $Gd_{55}Co_{25}Al_{18}Sn_2$ BMG. The critical exponents β and γ can be obtained from the A-N plots to be about 0.452 and 1.66, respectively. Thus the calculated value of n ($n_{\rm cal}$) can be obtained to be about 0.74, which is close to the value near $T_{\rm c}$ of the master curve proposed by Franco *et al.*, while is obviously different from the value directly obtained from the $\ln(-\Delta S_{\rm m}^{\rm peak})$–$\ln H$ plots.

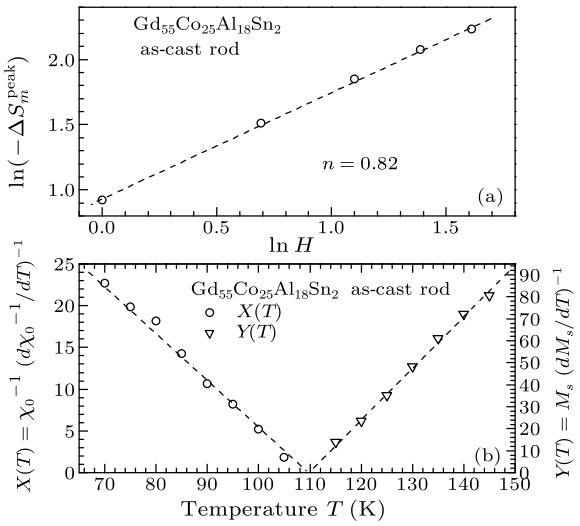

Fig. 4. (a) The $\ln(-\Delta S_{\rm m}^{\rm peak})$–$\ln H$ plots of the $Gd_{55}Co_{25}Al_{18}Sn_2$ as-cast rod, (b) the Kouvel–Fisher construction for determining the critical exponents.

The difference between n and $n_{\rm cal}$ is considered to be due to the microstructure of the BMGs being much more complicated than that of a single phase alloy because of the presence of short-range order (SRO), medium-range order (MRO) or even nano-crystallized (NC) structures embedded in the disordered matrix. In fact, we have found that the instantaneous slope of the $\ln(-\Delta S_{\rm m}^{\rm peak})$–$\ln H$ curve decreases continuously from about 0.921 under 1 T to about 0.767 under 5 T. The instantaneous slope of $\ln(-\Delta S_{\rm m}^{\rm peak})$–$\ln H$ is very close to $n_{\rm cal}$ under 5 T while it becomes larger with a decreased magnetic field, which is considered to be induced by the obstructed magnetization of the rod under low magnetic field due to the presence of the SRO, MRO, or NC structures.

In summary by minor Sn substitution for Al in $Gd_{55}Co_{25}Al_{20}$ BMG, we have obtained the $Gd_{55}Co_{25}Al_{18}Sn_2$ BMG with enhanced MCE. The values of $M_{\rm s}$ (about 208.0 A·m^2/kg), $-\Delta S_{\rm m}^{\rm peak}$ (about

9.32 J·kg^{-1}·K^{-1}) and R_C (about 832 J·kg^{-1}) of the $Gd_{55}Co_{25}Al_{18}Sn_2$ BMG are higher than those of $Gd_{55}Co_{25}Al_{20}$ BMG indicating the enhanced MCE by minor Sn addition. It is considered that the enlarged $\mu_{\rm eff}$, which indicates the strengthened $3d$–$4f$ interaction by minor Sn addition, appears to be the mechanism for the improved MCE of $Gd_{55}Ni_{25}Al_{18}Sn_2$ BMG. The field dependence of $-\Delta S_{\rm m}^{\rm peak}$ for the $Gd_{55}Co_{25}Al_{18}Sn_2$ BMG follows a $-\Delta S_{\rm m}^{\rm peak} \propto H^n$ ($n = 0.82$) relationship near $T_{\rm c}$, which is similar to the situation of other BMGs. The difference of n and $n_{\rm cal}$ is supposed to be induced by the obstructed magnetization of the BMGs under a low magnetic field due to the presence of the SRO, MRO, or NC structures.

References

[1] Tegus O, Bruck E, Buschow K H J and Boer F R D 2002 *Nature* **415** 150
[2] Pecharsky V K and Gschneidner J K A 1999 *J. Appl. Phys.* **200** 44
[3] Gschneidner J K A, Pecharsky V K and Tsokol A O 2005 *Rep. Prog. Phys.* **68** 1479
[4] Johnson W L 2002 *JOM* **54** 40
[5] Wang W H, Dong C and Shek C H 2004 *Mater. Sci. Eng.* **R44** 45
[6] Suryanarayana C and Inoue A 2011 *Bulk metallic Glasses* (Boca Raton: CRC Press)
[7] Inoue A and Takeuchi A 2011 *Acta Mater.* **59** 2243
[8] Pecharsky V K and Gschneidner J K A 1997 *Phys. Rev. Lett.* **78** 4494
[9] Hu F X, Shen B G and Sun J R 2000 *Appl. Phys. Lett.* **76** 3460
[10] Annaorazoy M P and Nikitin S A 1996 *J. Appl. Phys.* **79** 1689
[11] Luo Q, Zhao D Q, Pan M X and Wang W H 2006 *Appl. Phys. Lett.* **89** 081914
[12] Liang L, Hui X, Wu Y and Chen G L 2008 *J. Alloys Compd.*. **457** 541
[13] Liu Y S, Zhang J C and Wang Y Q 2009 *Appl. Phys. Lett.* **94** 112507
[14] Yuan F, Du J and Shen B L 2012 *Appl. Phys. Lett.* **101** 032405
[15] Wang P, Chan K C, Lu S, Tang M B and Xia L 2012 *Chin. Phys. Lett.* **29** 096103
[16] Atalay S, Gencer H and Kolat V S 2005 *J. Non-Cryst. Solids* **351** 2373
[17] Xu Z Y, Hui X, Wang E R, Chang J and Chen G L 2010 *J. Alloys Compd.* **504** S146
[18] Han J H, Mattern N, Schwarz B, Gorantla S, Gemming T and Eckert J 2012 *Intermetallics* **20** 115
[19] Liang L, Hui X, Wu Y and Chen G L 2008 *J. Alloys Compd.* **457** 541
[20] Luo Q, Zhao D Q, Pan M X and Wang W H 2008 *Appl. Phys. Lett.* **92** 011923
[21] Ding D, Xia L, Yu Z H and Dong Y D 2008 *Chin. Phys. Lett.* **25** 3414
[22] Liu Y, Zhang J, Wang Y, Zhu Y, Yang Z, Chen J and Cao S 2009 *Appl. Phys. Lett.* **94** 112507
[23] Franco V, Blázquez J S and Conde A 2006 *Appl. Phys. Lett.* **89** 222512
[24] Xia L, Fang S S, Jo C L and Dong Y D 2006 *Intermetallics* **14** 1098
[25] Xia L, Chan K C, Liu L and Wang G 2008 *J. Phys. D: Appl. Phys.* **41** 225410
[26] Lu S, Tang M B and Xia L 2011 *Physica* B **406** 3398
[27] Hoppe J I and Chem J 1972 *Education* **49** 505
[28] Nobuhiro M and Takuya S 2015 *Accred. Qual. Assur.* **20** 115
[29] Tishin A M 2007 *J. Magn. Magn. Mater.* **316** 351
[30] Franco V, Blázquez J S, Conde C F and Conde A 2006 *Appl. Phys. Lett.* **88** 042505
[31] Franco V, Blázquez J S and Conde A 2006 *J. Appl. Phys.* **100** 064307
[32] Franco V, Borrego J M, Conde C F, Conde A, Stoica M and Roth S 2006 *J. Appl. Phys.* **100** 083903
[33] Oesterreicher H and Parker F T 1984 *J. Appl. Phys.* **55** 4334
[34] Franco V, Blázquez J S and Conde A 2006 *Appl. Phys. Lett.* **89** 222512
[35] Kouvel J S and Fisher M E 1964 *Phys. Rev.* **136** A1626
[36] Xia L, Guan Q, Ding D, Tang M B and Dong Y D 2014 *Appl. Phys. Lett.* **105** 192402